Malaysian Journal of Analytical Sciences (MJAS)



Published by Malaysian Analytical Sciences Societ

IN SILICO AND MS/MS-BASED APPROACHES TO INVESTIGATE PROTEIN-PROTEIN INTERACTION NETWORKS IN Staphylococcus aureus BIOFILM

(Pendekatan Berasaskan *In Silico* dan MS/MS Untuk Mengkaji Jaringan Interaksi Protein-Protein dalam Biofilem *Staphylococcus aureus*)

Nawal Zulkiply¹, Norfatimah Mohamed Yunus¹, Hamidah Idris², Wan Syaidatul Aqma Wan Mohd Noor³, Saiful Anuar Karsani⁴, Mohd Fakharul Zaman Raja Yahya¹*

¹Faculty of Applied Sciences, Universiti Teknologi MARA, 40450 Shah Alam, Selangor, Malaysia ²Faculty of Science and Mathematics, Universiti Pendidikan Sultan Idris, 35900 Tanjung Malim, Perak, Malaysia ³Faculty of Science and Technology, Universiti Kebangsaan Malaysia, 43600 Bangi, Selangor, Malaysia ⁴Institute of Biological Sciences, Faculty of Science, University of Malaya, 50603 Kuala Lumpur, Malaysia

*Corresponding author: fakharulzaman@uitm.edu.my

Received: 7 September 2023; Accepted: 7 May 2024; Published: 27 August 2024

Abstract

Staphylococcus aureus is a Gram-positive pathogen inhabiting soft tissues like the epidermis and nasal cavity. Currently, there is limited knowledge of the protein-protein interaction (PPI) networks in *S. aureus* biofilm. The present study aimed to characterize *S. aureus* proteins and their interaction networks using an *in silico* approach and to identify the proteins expressed in *S. aureus* biofilm using tandem mass spectrometry. Initially, a preliminary characterization of the PPI networks in *S. aureus* was conducted using the STRING 12.0 database. Subsequently, *S. aureus* biofilm was developed in a 6-well microplate and harvested at 6 h, 12 h, 18 h, and 24 h. The expression of proteins in *S. aureus* biofilm was determined using a combination of one-dimensional SDS-PAGE and HPLC-ESI-MS/MS. The *in silico* results demonstrated that 147 biological processes, 46 molecular functions, 17 cellular components, and 15 biological pathways were significantly enriched (*p* <0.05) in the PPI networks of *S. aureus*. *S. aureus* biofilm proteins identified from the SDS-PAGE gel bands, such as L-lactate dehydrogenase (quinone), chaperone protein DnaK, and serine hydroxymethyltransferase, corroborated the findings obtained from the preliminary *in silico* work. In conclusion, the formation of biofilm by *S. aureus* may involve complex PPI networks.

Keywords: biofilm, in silico, protein-protein interaction network, Staphylococcus aureus, tandem mass spectrometry

Abstrak

Staphylococcus aureus adalah patogen Gram-positif yang mendiami tisu lembut seperti epidermis dan rongga hidung. Pada masa ini terdapat pengetahuan terhad tentang rangkaian interaksi protein-protein dalam biofilm S. aureus. Kerja-kerja ini dilakukan untuk mencirikan protein S. aureus dan rangkaian interaksinya menggunakan pendekatan dalam siliko dan untuk mengenal pasti protein yang dinyatakan dalam biofilm S. aureus menggunakan spektrometri jisim tandem. Pencirian awal rangkaian interaksi protein-protein dalam S. aureus telah dilakukan menggunakan pangkalan data STRING 12.0. Kemudian, biofilm S. aureus telah dibangunkan dalam plat mikro 6-telaga dan dituai pada 6 jam, 12 jam, 18 jam dan 24 jam. Ekspresi protein dalam biofilm S. aureus

Zulkiply et al.: IN SILICO AND MS/MS-BASED APPROACHES TO INVESTIGATE PROTEIN-PROTEIN INTERACTION NETWORKS IN Staphylococcus aureus BIOFILM

ditentukan menggunakan gabungan SDS-PAGE satu dimensi dan HPLC-ESI-MS/MS. Keputusan kajian *in silico* menunjukkan bahawa terdapat 147 proses biologi, 46 fungsi molekul, 17 komponen selular, dan 15 laluan biologi didapati diperkaya dengan ketara (P<0.05) dalam rangkaian interaksi protein-protein *S. aureus*. Protein biofilm *S. aureus* yang dikenalpasti daripada jalur gel SDS-PAGE seperti L-lactate dehydrogenase (quinone), protein pendamping DnaK, dan serine hydroxymethyltransferase, mengesahkan penemuan yang diperoleh daripada kajian awal *in silico*. Kesimpulannya, pembentukan biofilm oleh *S. aureus* mungkin melibatkan rangkaian interaksi protein-protein yang kompleks.

Kata kunci: biofilem, in silico, jaringan interaksi protein-protein, Staphylococcus aureus, spektrometri jisim ganda

Introduction

Biofilm formation is a vital adaptation and survival mechanism widely utilized by some microorganisms. It initiates with cellular attachment to a surface, followed by multiplication, maturation, and synthesis of a polymeric extracellular matrix, microbial dispersion, and ultimately, colonization of new surfaces. Biofilms are organized microbial sessile cell populations bound to surfaces, comprising polysaccharides, DNA, and other components within a self-produced extracellular matrix [1]. They exhibit heightened resistance to antimicrobial agents, significantly impacting the treatment of biofilm-related pathogens. Typically, biofilms are highly heterogeneous due to the mixture of single-layer and multilayer cells [2, 3]. According to Chajęcka-Wierzchowska et al. [4], this heterogeneous property often contributes to the survival of biofilms during antimicrobial therapy.

One of the important biofilm-forming pathogens is Staphylococcus aureus, an aerobic-anaerobic, nonmotile, Gram-positive bacterium that is catalasepositive and does not form spores. In humans, this pathogen often causes life-threatening diseases such as endocarditis and toxic shock syndrome. Due to its role as a common etiological agent of food intoxications, understanding and investigating S. aureus is crucial for safeguarding food safety and preventing outbreaks of gastroenteritis, particularly given its prevalence in many countries worldwide as a cause of foodborne illnesses. Diagnostic procedures for S. aureus commonly include coagulase, hemolysins, thermostable deoxyribonuclease tests, PCR, ELISA, and ELFA [5]. Common surface proteins of S. aureus include Sdr proteins, which are cell wall-associated proteins characterized by large serineaspartate repeat domains that play a role in the adhesion process [6]. The subfamilies of Sdr protein in S. aureus, namely SdrC, SdrD, and SdrE, share a conserved

structural organization; however, only SdrC is essential for biofilm growth via homophilic interaction [7, 8]. Previous *in silico* work has demonstrated that several antigenic proteins of *S. aureus* possess multiple functional linkages in a complex protein-protein interaction (PPI) network [9].

Proteins rarely perform their functions in isolation. Instead, the coordination of diverse cellular processes arises from functional interactions among several proteins and other biomolecules. Therefore, understanding PPI networks is crucial to identify which groups of proteins form functional units and underlie a wide range of metabolic and developmental processes [10]. The PPI networks in S. aureus biofilm have partially been elucidated using an in silico approach [11]. Investigating these networks provides insights into the mechanisms underlying biofilm formation and offers potential targets for developing novel antimicrobial strategies to combat biofilm-associated infections. However, there is still a lack of information about networks associated with major metabolic pathways in S. aureus biofilm. Therefore, the present study aimed to characterize S. aureus proteins and their interaction networks using an *in silico* approach, and to identify the proteins expressed in S. aureus biofilm using SDS-PAGE combined with tandem mass spectrometry.

Materials and Methods

Preparation of proteome dataset

A list of all proteins (799 proteins) expressed in *S. aureus* was obtained from the World-2DPAGE Repository, while the FASTA sequences of all *S. aureus* proteins were downloaded from UniProtKB [9]. Antigenicity, subcellular localization, and functional categories of all *S. aureus* proteins were analysed using VaxiJen, CELLO2GO, and UniProtKB, respectively.

In silico analysis of protein-protein interaction networks

A protein-protein interaction network was constructed using the STRING database, where functional linkages were predicted based on neighbourhood, co-expression, fusion-fission events, text mining, occurrence, and physical interactions [12]. Topography, functional linkages, and hub proteins were analysed based on the constructed network. The predicted functional linkages based on protein co-expression were validated by analysing the whole-cell proteome expression using a combination of one-dimensional SDS-PAGE and HPLC-ESI-MS/MS.

Preparation of test microorganism

S. aureus ATCC 33592 obtained from Microbiology Laboratory, Faculty of Applied Sciences, UiTM Shah Alam, Selangor was grown at 37°C in tryptic soy broth. The bacterial density was adjusted to 0.7 at 600 nm for biofilm formation assay.

Microscopic analysis

S. aureus and glass coverslip were incubated in a 6-well microplate for 6 h, 12 h, 18 h, and 24 h at 37 °C. After incubation, glass coverslips were rinsed with distilled water and submerged in 1 % crystal violet solution for 10 min. Then, glass coverslips were blot dry at room temperature and observed under light microscopy at 100x magnification [13]. The microscopic analysis was performed in triplicates.

Whole-cell protein extraction

Staphylococcus aureus was grown in 6-well microplates for 6 h, 12 h, 18 h and 24 h at 37 °C. Then, whole-cell protein extraction was performed as previously described [12]. The nutrient medium containing stationary-phase planktonic cells was discarded whilst biofilm fraction was rinsed with distilled water twice to remove non-adherent cells. The biofilm fraction was then suspended in 1mL of 0.9 % NaCl and was scratched out from the wells. The solution was transferred into a 1.5mL microcentrifuge tube and centrifuged at 10000 rpm for 10 min at 4 °C. The supernatant was discarded, and the remaining pellet was vigorously dissolved in 1 mL of lysis buffer (25 mM Tris, 150 mM NaCl, 0.5 %

SDS) containing 0.01 mM PMSF, and then vortexed, before being incubated at 95 °C for 15 min in a heater block, followed by another centrifugation at 10000 rpm for 10 min at 4 °C. The resulting supernatant was kept at -20 °C until further use.

Acetone precipitation

Protein samples were kept on ice to minimize degradation. Two hundred fifty microliters of protein samples and 500 μL of cold acetone were transferred into 1.5 mL microcentrifuge tubes and incubated overnight at -20 °C. Samples were then centrifuged at 14,000 rpm for 15 min at 4 °C. The supernatants were discarded, and protein pellets at the bottom of the microcentrifuge tube were stored at -20 °C. Protein concentration was determined using the standard Bradford assay protocol.

SDS-PAGE

Protein samples were heated for 5 min in boiling water, cooled to room temperature, and loaded (10 μg) onto precast 10% NuPAGE® Bis-Tris gels (8x8 cm, 1.0 mm). Electrophoresis was conducted at 200 V for 60 min using the XCell SureLock Mini-Cell system (Invitrogen, Life Technologies). BenchMarkTM Protein Ladder (Novex®, Life Technologies) estimated molecular weights. Gels were stained with SimplyBlueTM SafeStain (Life Technologies) and visualized on the ChemiDocTM MP System (Bio-Rad). This experiment was conducted in triplicates. Selected protein bands were digested using trypsin, and proteins were identified using HPLC–ESI-MS/MS.

Trypsin digestion

Protein bands were excised, destained in 50:50 acetonitrile: dH_2O with 25 mM ammonium bicarbonate (three times), vacuum-dried, and stored at -20 °C. Then, $10 \mu L$ of trypsin digest solution ($12.5 \mu g/mL$ trypsin, $25 \mu M$ ammonium bicarbonate) was applied and incubated overnight at 37 °C with each gel slice. Digested peptides were isolated, dried with Speed-Vac concentrate, desalinated with C18 ZipTip (Millipore), and their concentration was measured using the NanoDrop spectrophotometer for subsequent MS/MS analysis.

HPLC-ESI-MS/MS

Peptides were separated on a Dionex EASY-Spray 75 $\mu m \times 10$ cm column packed with PepMap C18 3 μm , 100 Å (Thermo Fisher Scientific) using solvent A (0.1% formic acid) and solvent B (0.1% formic acid in 100% ACN) at a flow rate of 300 nL/min with a 60 min gradient in Dionex Ultimate 3000 RSLC nano system. Peptides were analysed on a Q Exactive instrument with an EASY nanospray source at an electrospray potential of 1.5 kV. Raw data files were processed and searched using Proteome Discoverer 2.1 or 2.2, followed by data searching using the Mascot algorithm to identify proteins. The entire procedure was conducted in triplicates.

Results and Discussion

In silico analysis and experimental validation

In the present study, *S. aureus* proteome was characterized in terms of antigenicity, subcellular localization, biological process, molecular function, and functional protein interactions using the *in silico* approach. The expression of characterized proteins and the PPI networks in *S. aureus* biofilm was further verified using a combination of 1D SDS-PAGE and HPLC-ESI-MS/MS. The approach taken in the present study agrees with Rao et al. [14] stating that *in silico* data obtained from the prediction of PPI networks can be verified by various experimental methods including a combination of SDS-PAGE and mass spectrometry.

Antigenicity of protein

A total of 497 S. aureus proteins (62%) were predicted antigenic proteins, including enolase, phosphomevalonate kinase, elongation factor Tu, chaperone protein DnaK, catabolite control protein A and serine hydroxy methyltransferase. S. aureus presents a unique challenge for vaccine development. Moreover, the emergence of antibiotic-resistant strains of S. aureus has led to significant economic loss and ineffective treatment in hospitalised patients. As a result, there is a need for the creation of a vaccine that protects against S. aureus [15]. For a vaccine strategy to be effective, the vaccine must contain antigens that are expressed in the host microenvironments and elicit immune responses in humans. Identifying all those antigens that are recognized by the human immune system is a prerequisite for the selection of candidates for the development of a potent subunit vaccine. Potential vaccine candidate antigens must be present in the genome of circulating isolates, highly conserved, and expressed by S. aureus during natural infection. In a previous study, adding S. aureus protein antigens to a capsular conjugate vaccine enhanced its efficacy in the prevention and treatment of experimental S. aureus osteomyelitis in rats [16].

Subcellular localization

Figure 1 shows the prediction of subcellular localization of protein expressed in *S. aureus*. Cytoplasmic (93.74%) was predicted to be the major subcellular localization, followed by extracellular (4.38%), membrane (1.75%) and cell wall (0.13%).

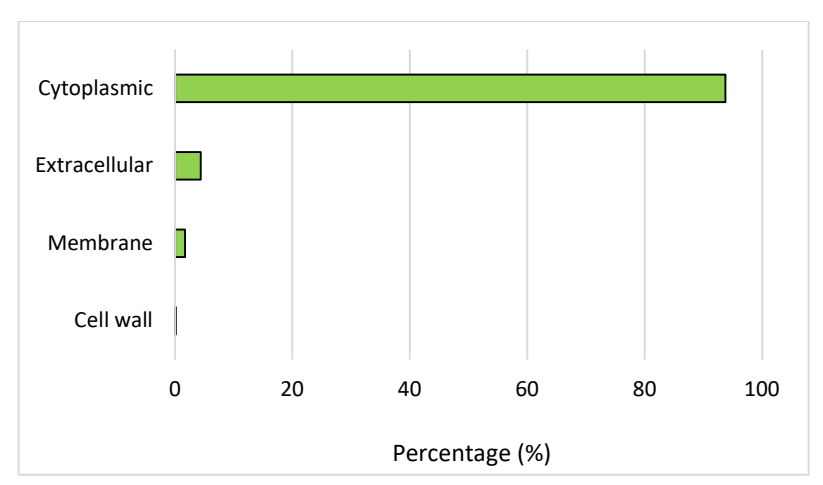


Figure 1. Subcellular localization of S. aureus proteins

A protein's subcellular localisation can give important information about its function. Knowledge of subcellular localisation of proteins in a cell is required to disclose the complicated pathways at the cellular level. In the present study, a total of 749 *S. aureus* proteins were predicted to be cytoplasmic including UDP-galactose 4-epimerase, phosphomevalonate kinase, ferrichrome transport ATP-binding protein and probable

N-acetylglucosamine-6-phosphate deacetylase. Most of the cytoplasmic proteins are involved in cellular metabolism. Thus, proteins

localized in the cytoplasm represent potential therapeutic targets [17].

Biological process

Based on Figure 2, 335 proteins (42%) of *S. aureus* were found to be involved in the cellular processes, 320 proteins (40%) in metabolic, 56 proteins (7%) in biological regulation, and 40 proteins (5%) in response stimulus. Other proteins were found to be involved in localization (24%), signalling (16%), and developmental process (8%).

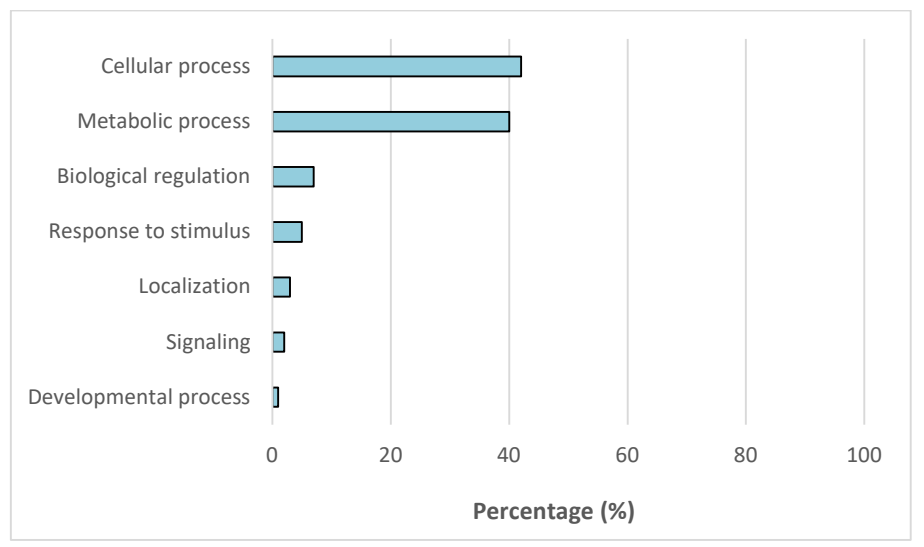


Figure 2. Function classification of *S. aureus* proteins based on biological process

S. aureus proteins involved in the cellular processes include glucokinase, cell division protein FtsA, citrate synthase and GTP-sensing transcriptional pleiotropic repressor CodY. The enzymatic reaction mediated by glucokinase is an energy-consuming mechanism. S. aureus is known to preserve energy by decreasing the expression level of this enzyme to suppress glycolysis [18].

Protein-protein interaction networks

A total of 799 *S. aureus* proteins were used as input data in the STRING database. Out of this number, only 437 proteins were successfully identified in the STRING database for the construction of PPI networks as the information on *S. aureus* proteome is incomplete in the STRING database. A total of 430 nodes and 958 functional interactions were produced in the network

(Figure 3). Meanwhile, the clustering coefficient value was predicted to be 0.411.

STRING is an online analysis tool used to analyse PPI networks which are often depicted as graphs, with nodes representing the various proteins and edges representing the physical interactions between proteins. In a scale-free network, most proteins participate in just a few interactions (referred to as 'nodes'), but a few proteins (referred to as 'hubs') participate in more than 10 functional interactions, showing that a few hubs bind many tiny nodes. The node diameter represents the network's degree parameter, which represents the number of connections formed by the nodes [19]. Nodes with a higher degree are more vital in the network since removing these nodes will cause the network to collapse [20]. In this study, complex functional interactions in *S*.

aureus were demonstrated. The PPI networks of different metabolism pathways in methicillin-resistant *S. aureus* (MRSA) have previously been reported [21]. On the other hand, average clustering coefficient measures the degree of interconnectivity in the neighbourhood of a node. It shows the overall tendency of nodes to form clusters. According to Hao et al. [22],

topological measures of network density such as the clustering coefficient is influenced by hub proteins. The high clustering coefficient values shown in the present study (>0.4) may promote cell self-organization in the natural networks, which are important to make cells more robust to perturbation [23].

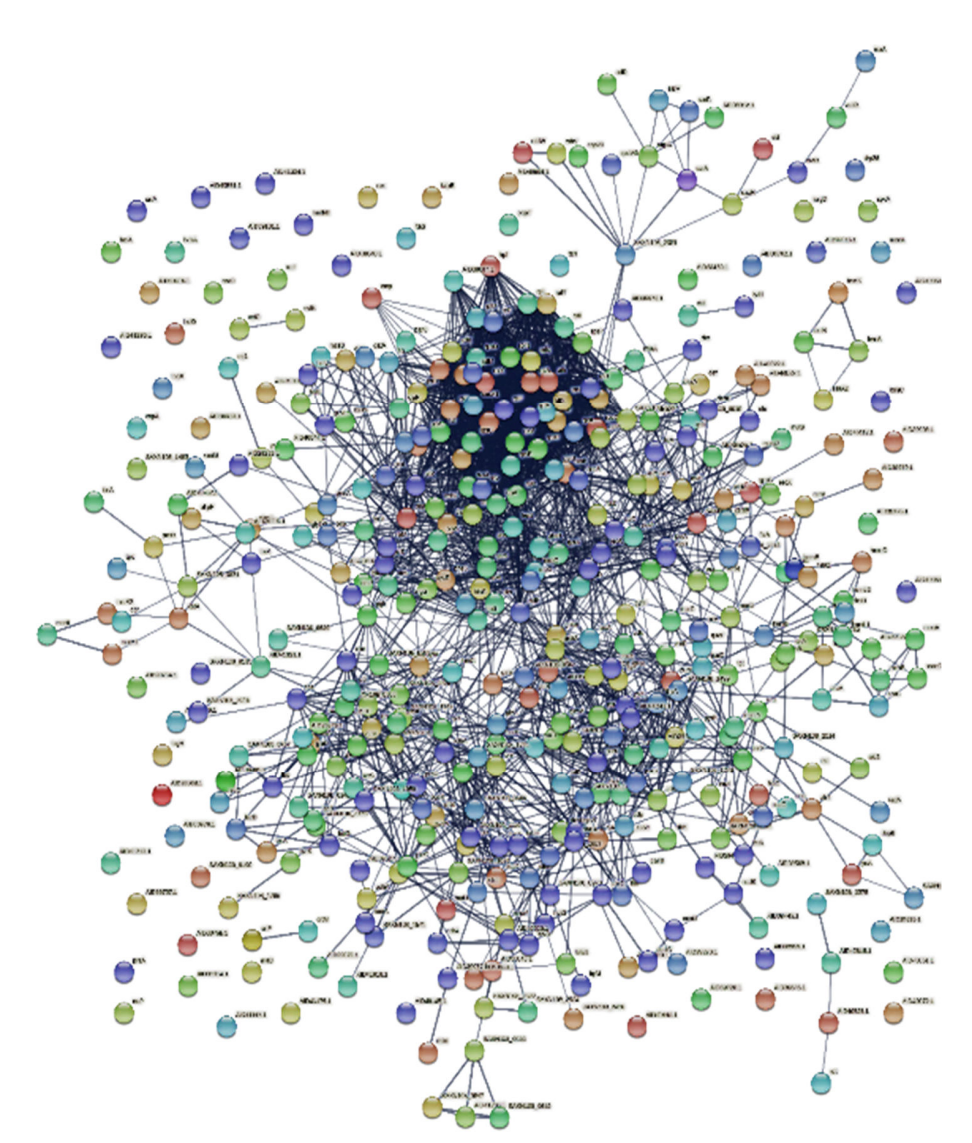


Figure 3. Functional interactions among S. aureus proteins

Hub proteins in S. aureus

There were 421 (96 %) proteins predicted as hub proteins as they showed more than 10 functional interactions with other proteins in the network,

including 50S ribosomal protein L21, elongation factor Tu and uridine kinase. Hubs, by definition, bind to many proteins. Previously, proteins with high connectivity were shown to interact to proteins with low connectivity,

and they typically bind to proteins from the same evolutionary period. These proteins play critical roles in closely linked subnetworks related to specific biological processes [24]. Hub proteins in the PPI network of MRSA represent new attractive drug development opportunities, as the discovery of specific inhibitors has the potential to expand our arsenal of antibiotics that may help address the problem of increasing antibiotic resistance [25]. It has been understood that the PPI network provides multiple drug targets, which are often sufficient to control diseases. According to Csermely et al. [26], drugs with multiple targets have a better chance of affecting the complex equilibrium of whole cellular networks than drugs that act on a single target.

Functional enrichment

A total of 147 biological processes, 46 molecular functions, 17 cellular components and 15 biological

pathways were significantly (P<0.05) enriched in the PPI networks of S. aureus. Table 1 shows the enriched biological processes, including the cellular nitrogen compound metabolic process, small molecule metabolic process, gene expression, and aromatic compound biosynthetic process. Table 2 shows the enriched molecular functions in S. aureus, including catalytic activity, binding, and transferase activity. Table 3 shows enriched cellular components including cellular anatomical entity, intracellular, cytoplasm and cytosol. Cellular anatomical entity and intracellular were the most predominant cellular component. Table 4 shows the enriched Kyoto Encyclopedia of Genes and Genomes (KEGG) pathways including metabolic pathways, biosynthesis of secondary metabolites, microbial metabolism in diverse environments and carbon metabolism.

Table 1. Representative enriched biological processes in S. aureus

Functional Enrichment	P-value	
Biological process		
Nitrogen compound metabolic process	7.97E ⁻³⁷	
Organic substance biosynthetic process	$1.00E^{-36}$	
Gene expression	$3.76E^{-18}$	
Translation	3.65E ⁻¹⁶	
Ribose phosphate metabolic process	$2.72E^{-14}$	
Carbohydrate derivative metabolic process	7.89E ⁻¹⁴	
Nucleic acid metabolic process	$2.10E^{-05}$	
Carbohydrate metabolic process	$9.54E^{-05}$	
ATP metabolic process	1.90E ⁻⁰³	
Glycolytic process	$4.20E^{-03}$	
RNA modification	1.25E ⁻⁰²	
Glucose metabolic process	$1.44E^{-02}$	
Lipid biosynthetic process	$1.44E^{-02}$	
RNA biosynthetic process	1.65E ⁻⁰²	
Cellular lipid metabolic process	$3.04E^{-02}$	
Cellular response to stress	3.65E ⁻⁰²	

Table 2. Representative enriched molecular functions in *S. aureus*

Functional Enrichment P-value					
Functional Enrichment					
Molecular function					
Heterocyclic compound binding	1.41E ⁻²²				
Small molecule binding	5.00E ⁻¹⁷				
Nucleotide binding	5.25E ⁻¹⁶				
Ion binding	1.85E ⁻¹⁵				
Carbohydrate derivative binding	7.24E ⁻¹⁴				
Adenyl nucleotide binding	2.88E ⁻¹²				
ATP binding	3.18E ⁻¹²				
RNA binding	1.49E ⁻¹⁰				
Ligase activity	1.78E ⁻¹⁰				
Nucleic acid binding	1.26E ⁻⁰⁷				
Transferase activity	$9.92E^{-07}$				
Metal ion binding	$1.27E^{-06}$				
GTP binding	$2.07E^{-02}$				
Zinc ion binding	$2.97E^{-02}$				
Ribonucleoprotein complex binding	4.21E ⁻⁰²				
Oxidoreductase activity, acting on a sulfur group of donors	4.61E ⁻⁰²				
Kinase activity	4.62E ⁻⁰²				

Table 3. Representative enriched cellular components in S. aureus

Functional Enrichment	P-value
Cellular component	
Intracellular	4.35E ⁻⁷⁰
Cytoplasm	5.36E ⁻⁵⁹
Cellular anatomical entity	2.47E ⁻³²
Cytosol	1.55E ⁻³¹
Protein-containing complex	5.68E ⁻¹¹
Ribosomal subunit	7.50E ⁻⁰⁷
Ribosome	1.23E ⁻⁰⁶
Cytosolic ribosome	1.23E ⁻⁰⁶
Organelle	1.23E ⁻⁰⁶
Intracellular organelle	1.68E ⁻⁰⁶
Intracellular non-membrane-bounded organelle	$2.34E^{-06}$
Large ribosomal subunit	4.55E ⁻⁰⁵
Cytosolic large ribosomal subunit	6.64E ⁻⁰⁵
Catalytic complex	2.00E ⁻⁰³
Small ribosomal subunit	1.60E ⁻⁰²
Cytosolic small ribosomal subunit	2.10E ⁻⁰²
Proton-transporting ATP synthase complex	3.36E ⁻⁰²

Table 4. Representative enriched biological pathways in S. aureus

Functional Enrichment	P-value
KEGG Pathway	
Metabolic pathways	1.80E ⁻¹⁵
Biosynthesis of secondary metabolites	1.39E ⁻⁰⁸
Aminoacyl-tRNA biosynthesis	9.99E ⁻⁰⁷
Ribosome	$8.20E^{-06}$
Microbial metabolism in diverse environments	$2.29E^{-05}$
Carbon metabolism	$2.29E^{-05}$
One carbon pool by folate	$2.20E^{-03}$
Glycolysis / Gluconeogenesis	$2.60E^{-03}$
Purine metabolism	$2.60E^{-03}$
Pyruvate metabolism	1.11E ⁻⁰²
Pentose phosphate pathway	1.56E ⁻⁰²
Arginine and proline metabolism	$1.74E^{-02}$
D-Alanine metabolism	$2.51E^{-02}$
Methane metabolism	$2.62E^{-02}$
Citrate cycle (TCA cycle)	4.05E ⁻⁰²

In this study, the rank-based Gene Ontology (GO) term enrichment of PPI networks identified biological processes and molecular function annotations associated with *S. aureus* proteins. The selection criterion was p-value; the closer the values were to zero, the more significant the enrichment. Enriched biological processes, such as cellular metabolic process, and

translation in the PPI networks of *S. aureus* have previously been reported [27].

Surface coverage of biofilm

Figure 4 shows the images of biofilm formation by *S. aureus* on glass coverslips under light microscope at 100x magnification. The surface coverage increased with increasing incubation time.

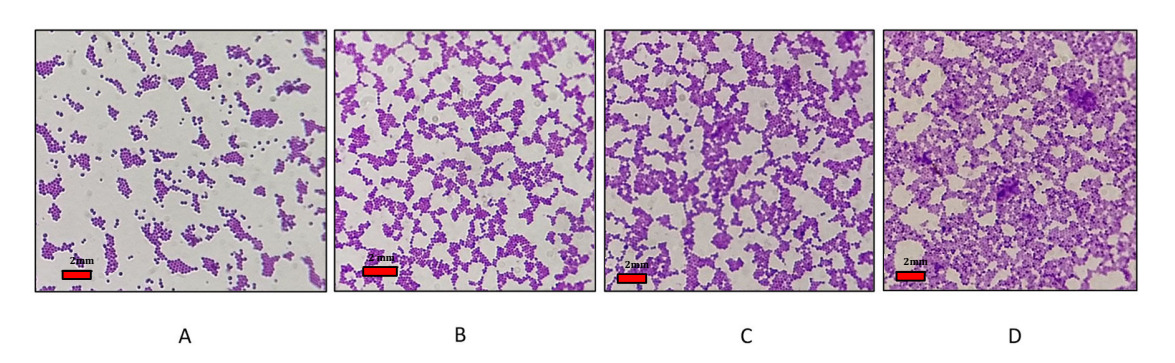


Figure 4. Formation of *S. aureus* biofilm on glass coverslip under light microscope (100x magnification). A) 6 h; B) 12 h; C) 18 h; D) 24 h

Light microscope images depicted the structure of biofilm architecture. The formation of biofilm began

with the attachment of free-floating microorganisms to surfaces leading to formation of a sessile population.

Biofilms were then observed to adhere to the surface of glass coverslips and form thick aggregates. The observation shown in the present study agrees with Bai et al. [13] who also observed the clumping of complex biofilm under a light microscope.

Proteome profile of S. aureus biofilm

Figure 5 shows the protein profile of *S. aureus* biofilm at different incubation periods. The longer incubation period showed more protein bands in *S. aureus* biofilm.

Major protein bands in each biofilm stage were as follows: 6 h – 36 kDa, 26 kDa; 12 h: 47 kDa, 37 kDa; 18 h: 47 kDa, 36 kDa, 33 kDa; 24 h: 80 kDa, 60 kDa, 58 kDa, 47 kDa, 35 kDa, 32 kDa, 30 kDa, 19 kDa. Protein bands of 27 kDa and 36 kDa were found to be expressed in 6h biofilm but no other biofilm stages. Protein bands of 80 kDa, 60 kDa, 58 kDa, 47 kDa, 35 kDa, and 32 kDa expressed in 24 h biofilm were selected for protein identification using MS/MS as they were found to be consistent across all experimental replicates.

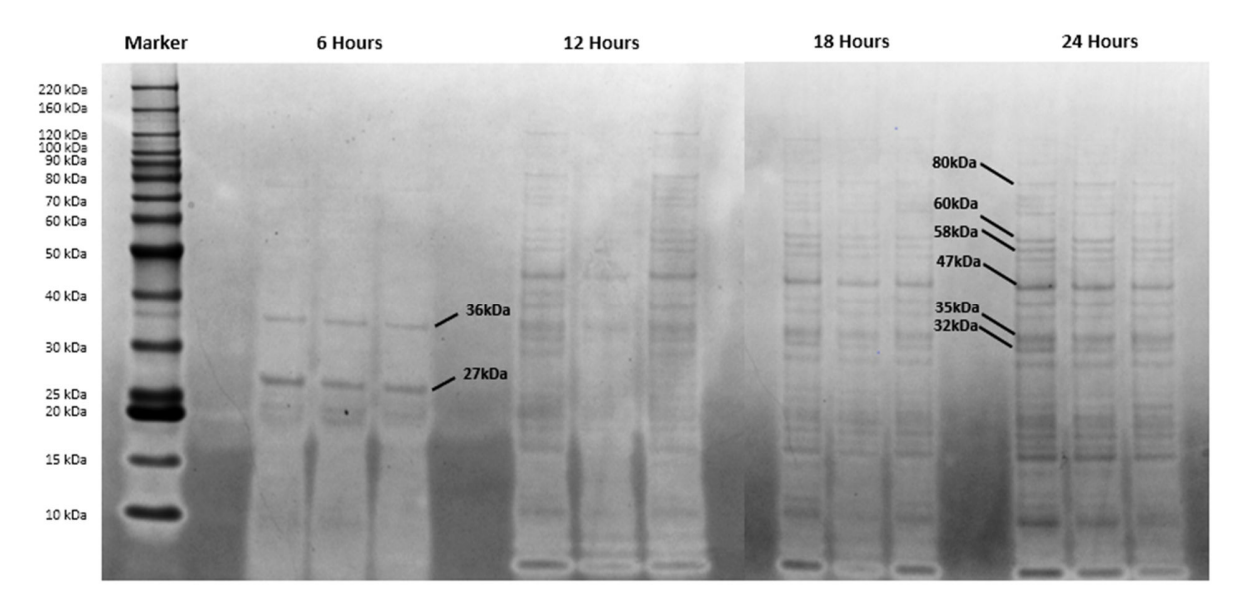


Figure 5. Whole cell protein expression in S. aureus biofilm at 6 h, 12 h, 18 h, and 24 h

One-dimensional SDS-PAGE is widely acknowledged as a useful technique for separating all types of proteins, including hydrophobic and low-molecular-mass proteins. The use of this approach in biofilm research is vital since biofilms comprise a diverse spectrum of hydrophobic proteins [12]. SDS-PAGE analysis was successfully used to obtain the whole-cell protein profile of *S. aureus* biofilm in the present study. Protein bands of *S. aureus* biofilm detected in the range between 25 – 80 kDa herein have also been reported elsewhere [28]. The banding pattern of *S. aureus* biofilm proteins was slightly changed across different developmental stages (6 – 24 h). This finding is in line with Lee et al. [29] who

found that the protein banding pattern of *Vibrio vulnificus* biofilm slightly changes due to the different heat shock conditions.

MS/MS-based identification of *S. aureus* biofilm proteins

Based on Table 5, a total of 55 proteins were identified in the 24 h biofilm. Of these, 18 identified proteins were previously characterized in the preliminary *in silico* analysis including enolase, protein translation elongation factor G, citrate synthase, and isocitrate dehydrogenase.

Table 5. A list of *S. aureus* proteins expressed in 24 h biofilm. The biofilm proteins characterized in the preliminary *in silico* analysis are indicated by (*)

-			- ,	,		
QUERY ACCESSION	MASCOT SCORE	PEPTIDE MATCH	SEQUENCE COVERAGE	PROTEIN NAME	E-VALUE	% IDENTITY
80kDa-57kDa						
P65424 *	109	6	13.05	L-lactate dehydrogenase (quinone)	0	99.80
A7WYS8	31	1	2.42	lysyl-tRNA synthetase	0	100.00
Q2FK44	18	1	2	formate C-acetyltransferase	0	100.00
T1YCX2 *	116	3	10.18	Malate:quinone oxidoreductase	0	100.00
A0A1Q8DF98	32	1	3.46	2-oxo acid dehydrogenase subunit E2	0	100.00
A0A033UQ54	27	1	1.98	ATP synthase subunit alpha	0	100.00
A0A033V5S8 *	14	1	0.95	carbamoyl-phosphate synthase large chain	0	100.00
A1A766 *	147	11	29.31	chaperone protein DnaK	0	57.69
A4WDC0 *	59	3	10.31	serine hydroxymethyltransferase	$1.00E^{-158}$	57.66
A0A133Q6X4 *	62	3	5.76	enolase	$7.00E^{-06}$	100.00
P64028 *	122	4	12.18	protein translation elongation factor G	$2.00E^{-07}$	100.00
O68883 *	217	5.00	14.75	citrate synthase	3.00E ⁻¹¹	100.00
P08200 *	41	3	12.02	isocitrate dehydrogenase [NADP]	$6.00E^{-179}$	63.57
47kDa-32kDa						
A7X0T9	79	6	6.45	Bifunctional autolysin	0	100.00
Q6GDG7	61	2	5.35	Arginine deiminase	0	100.00
Q2YU83	60	2	6.84	Bi-component leukocidin LukGH subunit H	0	100.00
Q2YSE8	57	5	11.29	Phosphopyruvate hydratase	0	100.00
P78386	56	2	4.93	Hypothetical protein	3.00E ⁻²⁴	63.75
Q2YVT4	54	2	4.18	Autolysin/adhesin Aaa	$2.00E^{-148}$	99.67
P99063	51	3	13.23	Alpha-ketoacid dehydrogenase subunit beta	0	99.69
Q6G723	47	1	5.95	CHAP domain-containing protein	$7.00E^{-107}$	99.26
Q2YXZ4	43	1	3.10	Glycine glycyltransferase FemB	0	100.00
P63871	40	4	13.55	TPA: cysteine synthase A	0	99.35
Q6GE15	40	2	6.41	Immunoglobulin-binding protein Sbi	0	100.00
Q2FZ75	36	1	4.44	Aspartate carbamoyltransferase catalytic subunit	0	100.00
Q4L6B1	31	1	2.06	Toxic anion resistance protein	0	92.54
B7JX26 *	26	1	3.79	S-adenosylmethionine synthase	5.00E ⁻¹⁷²	59.85
B0UWL1	22	1	4.79	Recombinase RecA, partial	4.00E ⁻¹⁵³	73.78
P68820 *	21	2	6.31	Phosphoglycerate kinase	0	100.00
O86793	21	1	2.94	tRNA	1.00E ⁻⁷⁵	49.38

Zulkiply et al.: IN SILICO AND MS/MS-BASED APPROACHES TO INVESTIGATE PROTEIN-PROTEIN INTERACTION NETWORKS IN Staphylococcus aureus BIOFILM

Q2FXM9 *	20	2	3.76	Pyruvate kinase	0	100.00
Q2YXZ5	19	1	4.52	Factor essential for expression of methicillin resistance	0	100.00
A6U4Y2 *	19	3	10.66	L-lactate dehydrogenase	0	100.00
Q6GAU2	16	1	4.11	Beta-ketoacyl-ACP synthase II	0	100.00
Q56194 *	18	2	3.65	Catabolite control protein A	0	83.89
Q2FY06 *	20	1	6.02	GTPase Era	0	100.00
A0A0U1MF82 *	183	6	16.24	Elongation factor Tu	0	100.00
A0A0E1X6S7	176	6	6.96	Mmannosyl-glycoprotein endo-beta-N-acetylglucosaminidase	0	100.00
A0A0E1X9I3	149	2	3.77	N-acetylmuramoyl-L-alanine amidase Sle1	$2.00E^{-166}$	100.00
A0A0E0VM62	122	3	8.31	Beta-cyano-L-alanine synthase	$3.00E^{-177}$	99.68
A0A380DJ06	66	1	3.69	Acid phosphatase	0	100.00
Q9AFB0	59	1	6.29	Leukocidin S subunit	0	99.65
A0A7U7EZ63	49	3	6.25	Methionine adenosyltransferase	0	100.00
I0B738	47	1	5.82	ScaC, partial	$2.00E^{-85}$	100.00
A0A380DRF9	45	1	7.98	Lipoprotein, putative	$2.00E^{-96}$	100.00
A0A380DZ84	43	1	3.08	FemB, factor involved in methicillin resistance / Glycine interpeptide bridge formation	0	100.00
A0A0H3JYS2	42	1	4.58	Alpha/beta hydrolase	0	100.00
A0A0E0VSM0	34	1	3.40	F0F1 ATP synthase subunit beta	0	100.00
A0A033V625	31	1	2.00	Hypothetical protein V070_00476	0	100.00
A0A0U1MI53 *	29	1	4.32	Pyruvate dehydrogenase E1 component subunit alpha	0	100.00
A0A0E0VMF5	26	1	4.97	Hypothetical protein ST398NM01_0409	0	100.00
A0A1Q8DG34 *	24	1	3.32	HistidinetRNA ligase	0	100.00
A0A2S6DGJ5	23	1	3.87	Type I glyceraldehyde-3-phosphate dehydrogenase	0	100.00
A0A0D1IBE9	23	1	4.64	ABC transporter substrate-binding protein	0	100.00
A0A1Q8DCE4	21	1	3.22	tRNA (adenosine(37)-N6)- Threonylcarbamoyltransferase complex transferase subunit TsaD	0	100.00

HPLC-ESI-MS/MS data acquisition is nearly fully automated, which enables analysis in a high throughput mode leading to low variations, thus, improving the confidence of the results. Romeu et al. [30] have used this protein identification approach to determine the amount and the distribution of proteins expressed in cyanobacterial strains in planktonic and biofilm stages. In our study, one of MS/MS-identified proteins is enolase, which was consistently expressed in the 24 h biofilm. This finding suggests that enolase may be

helpful for *S. aureus* adhesion. This suggestion is supported by the fact that enolase functions as a surface sensing receptor and clumping factor, initiating surface colonization [31]. The significantly higher transcript level of enolase in the first hours of growth under biofilm conditions compared to growth under planktonic conditions suggests the importance of this gene for the first phase of biofilm growth, in which bacterial cells interact with the extracellular ligands of a host [32].

Protein-protein interaction networks of MS/MS-identified proteins

A total of 18 identified proteins of *S. aureus* biofilm were used as input data in the STRING database. Only 15 proteins were successfully identified in the STRING database for PPI network construction. Our results showed that 15 nodes and 13 functional interactions of nodes and functional interactions, respectively were produced in the network. Table 6 shows the GO

enrichment analysis. A total of 9 biological processes, 9 molecular functions, 2 cellular components and 5 KEGG pathways were significantly (P<0.05) enriched in the PPI networks of *S. aureus* biofilm. Several enriched biological processes, molecular function and cellular component revealed by the network (Table 6) appear to verify the findings obtained from the preliminary *in silico* analysis (Figure 3, Table 1).

Table 6. Functional enrichment of PPI networks constructed using MS/MS-identified proteins of *S. aureus* biofilm. The biological process, molecular function, cellular component, and pathway characterized in the preliminary *in silico* analysis are indicated by (*)

Functional Enrichment	P-value
Biological process	
Generation of precursor metabolites and energy *	$2.40E^{-04}$
Glycolytic process *	$2.40E^{-04}$
Ribonucleotide metabolic process *	$5.20E^{-04}$
Carboxylic acid metabolic process *	$2.20E^{-03}$
Organic substance catabolic process *	$7.20E^{-03}$
Cellular response to organic substance	1.18E ⁻⁰²
Small molecule metabolic process *	$1.28E^{-02}$
Organonitrogen compound metabolic process *	$1.29E^{-02}$
Cellular nitrogen compound metabolic process *	1.74E ⁻⁰²
Molecular Function	
GTPase activity	$2.07E^{-02}$
Purine ribonucleotide binding *	$2.07E^{-02}$
Purine ribonucleoside triphosphate binding *	$2.07E^{-02}$
Small molecule binding *	$2.07E^{-02}$
Anion binding *	$2.07E^{-02}$
Catalytic activity *	$2.34E^{-02}$
Ion binding *	$2.34E^{-02}$
Protein-containing complex binding	$3.28E^{-02}$
Translation elongation factor activity	3.53E ⁻⁰²
Cellular Component	
Intracellular *	$1.88E^{-02}$
Cytoplasm *	3.35E ⁻⁰²
KEGG Pathway	
Glycolysis / Gluconeogenesis *	$4.40E^{-04}$
Carbon metabolism *	$4.40E^{-04}$
Microbial metabolism in diverse environments *	$6.50E^{-04}$
Biosynthesis of amino acids	$7.20E^{-04}$
Biosynthesis of secondary metabolites *	$3.10E^{-03}$
Pyruvate metabolism *	$4.32E^{-02}$

Cherkasov et al. [25] systematically identified the PPI networks for the hospital-acquired MRSA-252 strain using a high-throughput pull-down strategy combined with quantitative proteomics. They identified 13,219 interactions involving 608 MRSA proteins and revealed highly connected hub proteins. Interestingly, many existing clinical and experimental antimicrobial targets in the PPI networks of S. aureus were found to occupy peripheral positions with relatively few interacting partners. The hub proteins identified in MRSA's PPI networks, essential for network integrity and stability, have largely been overlooked as drug targets. However, Cherkasov et al. [25] did not correlate the observed protein interaction networks with the MRSA biofilm stage. Kang et al. [11] reported PPI networks among differentially expressed genes in various biofilm stages of S. aureus, with GO results indicating enrichment in biological processes such as cell adhesion and pathogenicity. However, their study lacked comprehensiveness, utilizing only 32 differentially expressed genes to construct the network. Our study demonstrated enriched metabolic pathways in the PPI networks of S. aureus biofilm, including glycolysis, amino acid biosynthesis, secondary metabolite biosynthesis, and pyruvate metabolism. These findings provide the first evidence of a more comprehensive PPI network of S. aureus biofilm, potentially aiding in the identification of novel antimicrobial drug targets to control S. aureus infections.

General discussion

The PPI networks play a crucial role in understanding the pathogenic mechanisms of infectious agents. These networks elucidate the complex web of interactions between pathogen proteins and host proteins, shedding light on the molecular mechanisms underlying infection [35]. By mapping out these interactions, researchers can identify key virulence factors and host targets, offering insights into potential drug targets for therapeutic intervention [36]. The PPI networks also facilitate the prediction of protein functions and pathways, aiding in the characterization of novel virulence factors and their roles in pathogenesis [37]. Identification of drug targets based on the PPI networks for other biofilm-forming pathogens such as *Salmonella Typhi* [38], *Pseudomonas*

aeruginosa [39], and Vibrio parahaemolyticus [40] has also been reported.

Conclusion

Our in silico analysis has shown that the PPI networks in S. aureus involve various biological pathways and numerous hub proteins. Further MS/MS-based identification of S. aureus biofilm proteins, including Llactate dehydrogenase (quinone), malate: quinone oxidoreductase, carbamoyl-phosphate synthase large chain, and chaperone protein DnaK, corroborates the findings from the preliminary in silico analysis. This study is the first comprehensive effort to characterize the PPI networks of S. aureus biofilm, potentially aiding in drug and vaccine development. Future investigations into the specific protein complexes or pathways identified in these networks may enhance the development of targeted therapeutic strategies for virulence and antibiotic resistance. Furthermore, integrating proteomic data with other omics approaches, such as transcriptomics and metabolomics, could provide a comprehensive understanding of the molecular mechanisms underlying biofilm formation.

Acknowledgements

This research was funded by the Pembiayaan Yuran Penerbitan Artikel (PYPA), Universiti Teknologi MARA.

References

- 1. Evelhoch, S. R. (2020). Biofilm and chronic nonhealing wound infections. *Surgical Clinics of North America*, 100(4): 727-732.
- Yaacob, M. F., Murata, A., Nor, N. H., Jesse, F. F. S. and Yahya, M. F. Z. R. (2021). Biochemical composition, morphology and antimicrobial susceptibility pattern of *Corynebacterium pseudotuberculosis* biofilm. *Journal of King Saud University Science*, 33(1): 101225.
- 3. Rashid, S. A. A., Yaacob, M. F., Aazmi, M. S., Jesse, F. F. A. and Yahya, M. F. Z. R. (2022). Inhibition of *Corynebacterium pseudotuberculosis* biofilm by DNA synthesis and protein synthesis inhibitors. *Journal of Sustainability Science and Management*, 17(4): 49-56.

- Chajęcka-Wierzchowska, W., Gajewska, J., Zakrzewski, A.J., Caggia, C. and Zadernowska, A. (2023). Molecular analysis of pathogenicity, adhesive matrix molecules (MSCRAMMs) and biofilm genes of coagulase-negative staphylococci isolated from ready-to-eat food. *International Journal of Environmental Search and Public Health*, 20: 1375.
- 5. Pal, M., Ketchakmadze, D., Durglishvili, N., and Ketchakmadze, K. (2022). *Staphylococcus aureus*: A major pathogen of food poisoning: a rare research report. *Nutrition & Food Processing*, 5(1): 1-3.
- Foster, T. J. (2019). Surface proteins of Staphylococcus aureus. Microbiology spectrum, 7(4): 7-4.
- Pi, Y., Chen, W., and Ji, Q. (2020). Structural basis of *Staphylococcus aureus* surface protein SdrC. *Biochemistry* 59: 1465–1469.
- Barbu, E. M., Mackenzie, C., Foster T, J. and Höök, M. (2014). SdrC induces staphylococcal biofilm formation through a homophilic interaction. *Molecular Microbiology*, 94: 172–185.
- 9. Zulkiply, N., Ramli, M. E. and Yahya, M. F. Z. R. (2022). *In silico* identification of antigenic proteins in *Staphylococcus aureus*. *Journal of Sustainability Science and Management*, 17: 18-26.
- Burke, D. F., Bryant, P., Barrio-Hernandez, I., Memon, D., Pozzati, G., Shenoy, Aditi., Zhu, W., Dunham, A. S., Albanese, P., Keller. A., Scheltema, R. A., Bruce, J. E., Leitner, A., Kundrotas, P., Beltrao, P. and Elofsson, A. (2023). Towards a structurally resolved human protein interaction network. *Nature Structural & Molecular Biology*, 30: 216-225.
- Kang, X., Ma Q, Wang, G., Li, N., Mao, Y., Wang, X., Wang, Y. and Wang, G. (2022). Potential mechanisms of quercetin influence the ClfB protein during biofilm formation of *Staphylococcus aureus*. *Frontiers in Pharmacology*, 13: 825489.
- Yahya, M. F. Z R., Karsani, S. A. and Alias, Z. (2017). Subtractive protein profiling of Salmonella typhimurium biofilm treated with DMSO. The Protein Journal. 36(4): 286-298.
- 13. Bai, J. R., Zhong, K., Wu, Y. P., Elena, G. and Gao, H. (2019). Antibiofilm activity of shikimic acid

- against *Staphylococcus aureus*. Food Control, 95: 327-333.
- Rao, V. S., Srinivas, K., Sujini, G. N. and Kumar, G. N. (2014). Protein-Protein Interaction Detection: Methods and Analysis. *International Journal of Proteomics*, 2014: 147648.
- Thomas, S. and Doytchinova, I. (2021). In silico identification of the b-cell and t-cell epitopes of the antigenic proteins of Staphylococcus aureus for potential vaccines. Vaccine Design, 439-447.
- Lattar, S. M., Noto Llana, M., Denoël, P., Germain, S., Buzzola, F. R., Lee, J. C. and Sordelli, D. O. (2014). Protein antigens increase the protective efficacy of a capsule-based vaccine against Staphylococcus aureus in a rat model of osteomyelitis. Infection and Immunity, 82(1): 83-91.
- Prava, J., G, P. and Pan, A. (2018). Functional assignment for essential hypothetical proteins of Staphylococcus aureus N315. International Journal of Biological Macromolecules, 108: 765-774.
- Li, H., Huang, Y. Y., Addo, K. A., Huang, Z. X., Yu, Y. G. and Xiao, X.L. (2022). Transcriptomic and proteomic analysis of *Staphylococcus aureus* response to cuminaldehyde stress. *International Journal of Food Microbiology*, 382: 109930.
- Isa, S. F. M., Hamid, U. M. A. and Yahya, M. F. Z.
 R. (2022). Treatment with the combined antimicrobials triggers proteomic changes in *Pseudomonas aeruginosa-Candida albicans* polyspecies biofilms. *ScienceAsia*, 48(2): 215-222.
- Kumar, S., Suyal, D. C., Yadav, A., Shouche, Y. and Goel, R. (2020). Psychrophilic *pseudomonas helmanticensis* proteome under simulated cold stress. *Cell Stress and Chaperones*, 25(6): 1025-1032.
- 21. Kang, S., Kong, F., Liang, X., Li, M., Yang, N., Cao, X., Yang, M., Tao, D., Yue, X. and Zheng, Y. (2019). Label-free quantitative proteomics reveals the multitargeted antibacterial mechanisms of lactobionic acid against methicillin-resistant Staphylococcus aureus (MRSA) using SWATH-MS technology. Journal of Agricultural and Food Chemistry, 67(44): 12322-12332.

- 22. Hao, D., Ren, C. and Li, C. (2012). Revisiting the variation of clustering coefficient of biological networks suggests new modular structure. *BMC System Biology*, 6: 34.
- 23. Galeota, E., Gravila, C., Castiglione, F., Bernaschi, M. and Cesareni. G. (2015). The hierarchical organization of natural protein interaction networks confers self-organization properties on Pseudocells. *BMC System Biology*, 9: S3.
- 24. Ekman, D., Light, S., Björklund, A. K. and Elofsson, A. (2006). What properties characterize the hub proteins of the protein-protein interaction network of saccharomyces cerevisiae? *Genome Biology*, 7(6): 45.
- Cherkasov, A., Hsing, M., Zoraghi, R., Foster, L. J., See, R. H., Stoynov, N. and Reiner, N. E. (2011). Mapping the protein interaction network in methicillin-resistant *Staphylococcus aureus*. *Journal of Proteome Research*, 10(3): 1139-1150.
- Csermely, P., Ágoston, V. and Pongor, S. (2005).
 The efficiency of multi-target drugs: the network approach might help drug design. *Trends in Pharmacological Sciences*, 26(4): 178-182.
- 27. Tang, C., Chen, J., Zhang, L., Zhang, R., Zhang, S., Ye, S., Zhao, Z. and Yang, D. (2020). Exploring the antibacterial mechanism of essential oils by membrane permeability, apoptosis and biofilm formation combination with proteomics analysis against methicillin-resistant *Staphylococcus aureus*. *International Journal of Medical Microbiology*, 310(5): 151435.
- 28. Secor, P.R., James, G.A., Fleckman, P. et al. (2011). *Staphylococcus aureus* biofilm and planktonic cultures differentially impact gene expression, mapk phosphorylation, and cytokine production in human keratinocytes. *BMC Microbiology* 11: 143.
- Lee, K. J., Jung, Y. C., Park, S. J. and Lee, K. H. (2018). Role of heat shock proteases in quorum-sensing-mediated regulation of biofilm formation by *Vibrio* species. *American Society for Microbiology*, 9(1): 17.
- Romeu, M. J., Domínguez-Pérez, D., Almeida, D., Morais, J., Campos, A., Vasconcelos, V. and Mergulhão, F. J. (2020). Characterization of planktonic and biofilm cells from two filamentous

- cyanobacteria using a shotgun proteomic approach. *Biofouling*, 36(6): 631-645.
- 31. Kot, B., Sytykiewicz, H. and Sprawka, I. (2018). Expression of the biofilm-associated genes in methicillin-resistant *Staphylococcus aureus* in biofilm and planktonic conditions. *International Journal of Molecular Sciences*, 19(11): 3487.
- 32. Cattò, C., Villa, F. and Cappitelli, F. (2021). Understanding the role of the antioxidant drug erdosteine and its active metabolite on *Staphylococcus aureus* methicillin resistant biofilm formation. *Antioxidants*, 10(12): 1922.
- 33. Bonhomme, J., Chauvel, M., Goyard, S., Roux, P., Rossignol, T. and d'Enfert, C. (2011). Contribution of the glycolytic flux and hypoxia adaptation to efficient biofilm formation by *Candida albicans*. *Molecular Microbiology*, 80(4): 995-1013.
- 34. Othman, N. A. and Yahya M. F. Z. R. (2019). *In silico* analysis of essential and non-homologous proteins in *Salmonella typhimurium* biofilm. *Journal of Physics: Conference Series*, 1349: 012133.
- 35. Saha, S., Prasad, A., Chatterjee, P., Basu, S. and Nasipuri, M. (2018). Protein function prediction from protein–protein interaction network using gene ontology based neighborhood analysis and physico-chemical features. *Journal of Bioinformatics and Computational Biology*, 16(06): 1850025.
- 36. Loscalzo, J. (2023). Molecular interaction networks and drug development: Novel approach to drug target identification and drug repositioning. *The FASEB Journal*, 37(1): e22660.
- 37. Hanes, R., Zhang, F. and Huang, Z. (2023). Protein interaction network analysis to investigate stress response, virulence, and antibiotic resistance mechanisms in *Listeria monocytogenes*. *Microorganisms*, 11(4): 930.
- 38. Afzal, M., Hassan, S. S., Sohail, S., Camps, I., Khan, Y., Basharat, Z., ... and Morel, C. M. (2023). Genomic landscape of the emerging XDR Salmonella Typhi for mining druggable targets clpP, hisH, folP and gpmI and screening of novel TCM inhibitors, molecular docking and simulation analyses. *BMC Microbiology*, 23(1): 25.

- 39. Bajire, S. K., Ghate, S. D., Shetty, S., Banerjee, S., Rao, R. S. P., Shetty, V., and Shastry, R. P. (2023). Unveiling the role of hub proteins in controlling quorum sensing regulated virulence through analogues in Pseudomonas aeruginosa PAO1: A functional protein-protein network biology approach. *Biochemical and Biophysical Research Communications*, 660: 13-20.
- 40. She, W., Cheng, A., Ye, W., Zeng, P., Wang, H., and Qian, P. Y. (2023). Mode of action of antimicrobial agents albofungins in eradicating penicillin-and cephalosporin-resistant *Vibrio parahaemolyticus* biofilm. *Microbiology Spectrum*, 11(5): e01563-23.